Applied Catalysis B: Environmental 234 (2018) 365–377

Contents lists available at ScienceDirect

Applied Catalysis B: Environmental

journal homepage: www.elsevier.com/locate/apcatb

$CaSO_4$ deactivated V_2O_5-WO_3/TiO_2 SCR catalyst for a diesel power plant. Characterization and simulation of the kinetics of the SCR reactions

C.U. Ingemar Odenbrand

Department of Chemical Engineering, Lund University, P.O. Box 124, SE-221 00 Lund, Sweden

ARTICLE INFO

Keywords:
Ca deactivation
Vanadia SCR diesel catalyst
Poisoning and kinetics
Formation of N_2O

ABSTRACT

The deactivation of a diesel SCR (Selective Catalytic Reduction) catalyst by impregnation with $CaSO_4$ was studied. The loss in activity after 2729 h of use on the engine was lower than when deactivated by impregnation. This was the case even if the amount of Ca in the catalyst was high after use on the engine. In the used catalyst a surface layer of $CaSO_4$ was built up on the monolith during use. This causes lower deactivation than when $CaSO_4$ was introduced in the pore system of the catalyst.

The kinetics of the SCR reaction, the oxidation of NH_3 to N_2 and two side reactions leading to N_2O was used in the simulation. A coverage dependent heat of adsorption of NH_3 was used. The heat decreased with the coverage and with the introduction of $CaSO_4$ into the pores. After fitting the amounts of NO and N_2O at the exit of the reactor against the temperature at the exit of the bed excellent agreements were obtained for the products N_2 and H_2O as well for the reactant NH_3.

This is the first time that the effect of $CaSO_4$ poisoning of SCR catalysts and its effect on the kinetics is published.

1. Introduction

The Selective Catalytic Reduction (SCR) technique, for reduction of NO_x with ammonia, was originally invented in the early 60's, developed in Japan in the 70's and introduced in Europe in the 80's. From the beginning, the technique was used in large stationary boilers and nitric acid plants. Today the concept was developed further and comprises mobile applications like marine and automotive diesel engines. Marine engines are often run under conditions, which resembles the ones in stationary diesel power plants. In 2017 there are hundreds of SCR units installed on ships [1]. The SCR technique is not as selective as the name implies. N_2O is being formed, albeit in quiet low amounts, as a side reaction of the SCR on many different catalysts [2]. Because of its high value of the greenhouse effect N_2O has been regulated by law since 2015 [3]. We have studied catalyst applications for treating different compounds in diesel exhausts extensively. One early study [4] showed that it is possible to combust diesel soot catalytically at low temperatures. We also contributed to the early development of the SCR technology for use on trucks using urea as reducing agent [5]. In another paper, we published the effect of lead on the activity of SCR catalysts mainly used in municipal waste incinerators [6]. In 1996 a publication of the evaluation of the first SCR plants in Sweden, some of which were based on diesel engines, was published [7]. Kamata et al. [8] showed the effect of phosphorus on the acidity of the catalyst and on its activity since phosphorus is a common poison in diesel applications. Kamata et al. [9] also studied the effect of K_2O on the activity of a commercial V_2O_5-WO_3/TiO_2 SCR catalyst. This study was aimed at applications where forest residues we burnt to produce heat and power. We later studied the thermal stability of vanadia-based SCR catalysts for the use in diesel applications [10] since these catalysts could experience high temperatures during use. In a recent study of deactivations, we published data and a model for the deactivation by K, Na and Zn in a waste incineration plant [11].

The lubricating oil for the engine is often a source for deactivation components for the catalyst. A SAE 15 W-40 oil contained S 0.26, Ca 0.25, Zn 0.068 and P 0.061 wt. % [12]. Nicosia et al. [13] studied the deactivation by calcium, phosphate and potassium on V_2O_5/WO_3-TiO_2 catalysts for diesel systems. They showed that Ca ions (introduced as calcium acetate), at 0.4 mol% based on vanadium, decreased the conversion of NO from 98 to 65% at 400 °C. When SO_4^{2-} was present (introduced by feeding SO_2 at 400 °C for 5 h), the deactivation was almost unnoticeable. Kröcher and Elsener [14] studied more carefully the effect of lubricating oil components (Ca, Mg, Zn, P, B and Mo), impurities in diesel fuel (K from rapeseed methyl ester) and impurities in the urea solution (Ca and K) on the activity of vanadia based SCR catalysts. Single components (i.e. Ca as acetate) were used for catalyst impregnation. Similar effect as presented by Nicosia [13] was obtained for Ca. Nicosia et al. [15] characterized the deactivated catalysts by

E-mail addresses: Ingemar.odenbrand@chemeng.lth.se, ingemar.odenbrand@comhem.se.

https://doi.org/10.1016/j.apcatb.2018.03.063
Received 29 January 2018; Received in revised form 15 March 2018; Accepted 19 March 2018
Available online 15 April 2018
0926-3373/

NH_3-TPD and found that the fresh catalyst desorbed 3.4 mg/g NH_3 while Ca-poisoned one desorbed 2.0 mg/g. Thus, a decrease in the number of acid sites was proven. By using Diffuse Reflectance Infrared Fourier Transform Spectroscopy (DRIFTS) of adsorbed ammonia, it was possible to distinguish between Lewis and Brønsted acid sites. It was only the Brønsted sites that were affected by poisoning. Using Density Functional Theory (DFT) calculations they demonstrated that one calcium metal atom poisons 4 vanadium atoms.

The influence of phosphorous, alkaline and alkaline earth metals as well as Cu and Cr on SCR was studied, in a high-throughput study, by Klimczak et al. [16]. Effects of impurities in biodiesel (K, Na, P), in urea solution (K, Na, Ca, Mg) and components from abrasion of the engine (Cr, Cu) on catalyst activity were reported. Different methods for catalyst doping, i.e. impregnation and poisoning by aerosols were used. The results from impregnation with nitrates show that at a loading of 0.5 mmol/g washcoat the activity was decreased by 75% for Ca at 350 °C. When an aerosol from $Ca(NO_3)_2$ was introduced at 500 °C and the activity measured at 350 °C, a decrease in conversion by 23% was observed. The amount of adsorbed NH_3 was 1.9 ml/g for the fresh catalyst and 1.5 ml/g for the one containing Ca, i.e. a decrease in ammonia adsorption capacity by 21%. The effect of deposition by aerosols is thus much smaller than that using impregnation. Maunula et al. [17] studied SCR catalysts in mobile off-road applications. They found that the after 3 000 and 8 000 h aging catalysts had axial accumulation of the elements (P, Zn, Ca, Na, K, S, Si and Fe) coming from lubrication oil and fuel oil. Only the front part of the catalyst had higher concentrations of poisons, which correlate to the decreased conversion of NO_x.

There is not very much information in literature on the deactivation by calcium. Therefore, it is still need for more information on the deactivation of SCR catalysts by calcium in various applications and especially in the diesel application.

The aim of this study is to study the effect on activity and the formation of N_2O when $CaSO_4$ poisons the catalyst. We intend to show how an impregnation with aqueous solutions of $CaSO_4$*$2H_2O$ deactivates a commercial V_2O_5/WO_3-TiO_2 catalyst which was first pre-poisoned by use in a diesel power plants for 2729 h.

We also want to develop a static global kinetic model, which can fit the data obtained when the activity and selectivity of different, by $CaSO_4$, deactivated catalyst samples are measured in laboratory. Since these data are measured at different degrees of poisoning by Ca they could be used in the design of new catalysts for diesel engines which are deactivated on-line by Ca.

2. Experimental

2.1. Deactivation procedure

The catalyst, used in the investigations, was taken from an application in a diesel power plant. It most probably was from BASF and their high temperature version with about 0.5 wt% V_2O_5. The catalyst in the plant had a pitch of 3.7 mm, a wall thickness of 0.14 mm with a channel area of 870 m^2/m^3. The used catalyst was run for 2729 h in the diesel plant, so a certain amount of $CaSO_4$ was already found in the pore system.

The monoliths were crushed and sieved and the fraction between 0.425 and 0.800 mm was used for introducing extra Ca by impregnation with $CaSO_4$*$2H_2O$. Wet impregnation by an aqueous solution of calcium sulphate was used to introduce Ca to a number of samples from the catalyst used for 2729 h. However, the solubility of $CaSO_4$ in water is very low. It is almost independent of temperature between 0 and 100 °C and is around 2.5 g per l water [18].

After impregnation, the catalyst was left over night at room temperature. The catalyst was then dried at 50 °C under a flow of air. Then a temperature of 150 °C was used and the catalyst was flushed by air for 2 h.

For preparation of more poisoned catalyst samples, the whole process (wet impregnation + drying) was performed as many times in succession as needed. After each preparation, a small amount of poisoned catalyst was saved for the following investigations, and the remaining was treated in the same way and under the same conditions.

Table 1
Catalyst preparations.

Description	Method of preparation
Fresh catalyst	Not impregnated
Used	Used for 2729 h not impregnated
1 * unsaturated $CaSO_4$	0.53 g $CaSO_4$ in 500 ml water
1 *	1 time impregnated with saturated solution
2 *	2 times impregnated with saturated solution
3 *	3 times impregnated with saturated solution
5 *	5 times impregnated with saturated solution
7 *	7 times impregnated with saturated solution
1 * unsaturated $CaSO_4$	0.12 g $CaSO_4$*$2H_2O$ in 500 ml water

n.d. not measured by AAS.

All the prepared samples were investigated with regard to their behaviour in the SCR reaction. All preparations are listed in Table 1.

2.2. Measurement of catalyst activity

The activities of fresh and deactivated catalyst samples were determined with the same equipment as used before except for the reactor [6]. The catalytic reactor was made of quartz with an inside diameter of 10.5 mm. The reactor was heated by an oven and the reaction could be performed in a temperature range from 250 °C up to a maximum of 550 °C (Fig. 1). The reactant gases were supplied from cylinders with premixed gases of known compositions (around 1.5%) in a carrier gas of helium with 3000 ppm argon. The inlet gas stream contained 600 ppm NO, 700 ppm NH_3, and 2% O_2. The monoliths were crushed and sieved and 0.1 g of the fraction between 0.425 and 0.800 mm was used in the catalyst activity tests.

A Balzer QMG 311 mass spectrometer was used for gas analysis. A chopping device was used to decrease the influence of the background signal. The spectra were recorded using peaks 17, 18, 28, 30, 34, 40, 44 and 46 for NH_3, H_2O, N_2, NO, O_2, Ar, N_2O and NO_2. The spectrum was scanned twice first with an open and then with a closed chopper. By subtraction, a difference spectrum representing the composition in the gas stream was obtained. Experimentally determined splitting factors and sensitivity factors, determined from gases of known compositions, were used to calculate the concentrations with a computer program. The temperatures at which the activity was measured were from 250 to 550 °C at 25 °C intervals. An equilibration time of 20 min was used at each temperature. The flow rate was 900 Ncm^3/min, and the pressure was kept at about 1.25 bar. The inlet values were measured at 350 °C after 30 min' equilibration.

The activity is presented as a pseudo first order rate constant determined from the following equations:

$$r = -k*C_{NO}*a*C_{NH3}/(1 + a*C_{NH3})$$

is used in the simulations and is of the Eley-Rideal type.

For temperatures below 400 °C the adsorption factor for NH_3 is equal to 1 so the rate can be approximated by:

$r = -k*C_{NO}$ (mol/g/min)

x = ([NO]in-[NO]out)/[NO]in = conversion of NO

$k = -F_0$ /([NO]in*m_{cat})*ln(1-x) (rate constant per g of catalyst, cm^3/min/g)

$k = k_0*\exp(-E_a/(R*T))$ Arrhenius dependence of rate constant on temperature

[NO]in = Concentration of NO in inlet to reactor (mol/cm^3)

[NO]out = Concentration of NO in outlet from reactor (mol/cm^3)

k_0 = pre exponential factor (cm^3/min/g)

E_a = activation energy (J/mol)

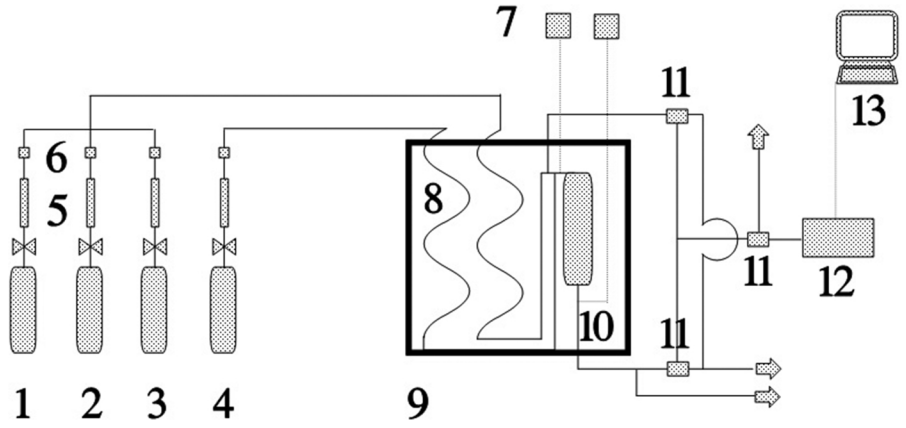

Fig. 1. Experimental setup. 1–4 = Gas cylinders for He, O_2, NO and NH_3, 5 = Rotameters, 6 = Flow regulators, 7 = Pressure sensors, 8 = Preheating quartz glass tubes, 9 = Oven with temperature regulator, 10 = Reactor of quartz glass, 11 = 3-way valves for choosing gas to analyser, 12 = Mass spectrometer, 13 = Computer.

R = gas constant (J/mol/K)
T = temperature (K)
m_{cat} = catalyst weight (g)
F_0 = molar flow of NO into the reactor (mol/min)
The selectivity for the formation of N_2O is defined as [19]:
Sel N_2O = N_2O formed/(N_2O formed + N_2 formed)

2.3. Surface area and pore structure analysis by N_2 adsorption

N_2 adsorption was performed on all samples used in this study with a Micromeritics ASAP 2400 equipment after outgassing at 0.04 Torr and 90 °C for 1 h and at 400 °C for 24 h to a final pressure of 10^{-3} Torr. Determination of the surface area and the pore size distribution was carried out by physisorption of N_2 at −196 °C. The accuracy of the method for measuring the BET surface area is around 1% as determined separately for the experimental conditions used.

2.4. Measurement of catalyst composition by AAS, XPS and SEM-EDAX

To determine the content of calcium, all catalyst samples were dissolved in a mixture of hydrofluoric acid (Merck 48%, p.A.) and nitric acid (Merck 68%, p.A.) in the proportion of 4:1. The following analysis of the calcium was performed by atomic absorption using a GBC 908 (Nord Lab Plus) atomic absorption spectrometer (AAS). The solutions were diluted with distilled water to the concentrations needed for analysis. All analyses were done with double or triple samples to lower the influence of analytical errors. The results shown are the mean values of the experimental ones in weight percent. SEM and XPS analysis was performed on the monolithic samples. The surface composition of the catalysts was analysed by XPS (X-ray Photoelectron Spectroscopy) using an electron-probe micro-analyser SEMQ (ARL) and a X-ray spectrometer KEVEX 5100 (Kevex, USA). The SEM equipment was a JEOL JSM-840-A scanning microscope with a Link AN 1000 energy-dispersive X-ray analyser. Various elements were determined quantitatively over the cross section of the catalyst monolith.

2.5. Temperature programmed desorption of NH_3

The temperature programmed desorption, TPD, experiments were conducted in an equipment consisting of a reactor made of quartz with a 4 mm inner diameter. A two-hundred mg sample was placed on a fritted glass filter in the reactor. The heating of the reactor was accomplished by a gold-lined quartz tubular oven from Trans. Temp. Co. (USA). The temperature was increased linearly by a Eurotherm 902 electronic controller. The effluent gases were analyzed using a VG Pegasus SC mass spectrometer, MS. The inlet system to the MS consists of a stainless steel capillary leaking sample gas from a flow of 50 cm^3/min through the reactor. All lines after the reactor were made of stainless steel tubing with an inner diameter of 2 mm and were heated to 150 °C. The mass spectrometer was calibrated regularly with standard gases of known composition (from Alfax AB). The adsorption gas contained 1.5% NH_3 in helium with 3 000 ppm Ar. The ProcessSoft program (from VG) was used during both the calibration and the measurement sequences. The following masses (m/e) were used: 44 (N_2O), 40 (Ar), 32 (O_2), 30 (NO), 28 (N_2), 18 (H_2O) and 17 (NH_3). During the calibration sequence both the sensitivity factors and the splitting factors were determined automatically by the program yielding quantitative analysis of the composition of the gas phase.

The TPD experiments were conducted as follows. The sample was degassed at 400 °C for one hour under a flow of 50 cm^3/min of helium. The sample was then cooled in a helium flow to 150 °C during one hour. Ammonia was adsorbed at 150 °C during 20 min. The physisorbed ammonia was desorbed at the same temperature by a flow of helium during one hour. Another adsorption/desorption sequence was then performed as above. The TPD was then started by increasing the temperature at a specified rate. The TPD experiments were done with the rates 15, 20 and 25 K/min. The outlet gases were analyzed with the mass spectrometer.

The results from the TPD experiments were only used to determine the effect of the ammonia coverage on its heat of desorption and are not presented here.

2.6. Modelling of the catalyst reactions

The kinetic scheme used in the simulations is based on reactions between adsorbed ammonia and gaseous nitric oxide according to an Eley-Rideal model [20] as shown in Table 2. All oxidation reactions of ammonia are also based on adsorbed ammonia. In all cases, the effect of oxygen, present in excess (2%), is included in the rate constant

Table 2
Chemical reactions and kinetic expressions used in the simulations.

Reaction	Global reaction	Rate expression
1	$4NO + 4NH_3 + O_2 => 4N_2 + 6H_2O$	$r_1 = A_1 * \exp(-E_1/(RT)) * C_{NO} * \theta_{NH3}$
2	$4NH_3 + 3O_2 => 2N_2 + 6H_2O$	$r_2 = A_2 * \exp(-E_2/(RT)) * \theta_{NH3}$
3	$4NO + 4NH_3 + 3O_2 => 4N_2O + 6H_2O$	$r_3 = A_3 * \exp(-E_3/(RT)) * C_{NO} * \theta_{NH3}$
4	$4NH_3 + 4O_2 => 2N_2O + 6H_2O$	$r_4 = A_4 * \exp(-E_4/(RT)) * \theta_{NH3}$
5	$4NH_3 + 5O_2 => 4NO + 6H_2O$	$r_5 = A_5 * \exp(-E_5/(RT)) * \theta_{NH3}$

$\theta_{NH3} = K_{NH3} * C_{NH3}/(1 + K_{NH3} * C_{NH3})$.

Table 3
Physical data used in the Heat Transfer in Porous Media and Free and Porous Media Flow nodes.

Parameters	Open channel	Catalyst layer	Wall
ε_{bed}	n.a.	0.4	n.a.
Θ_p	n.a.	0.6	n.a.
K (m^2)	n.a.	6.7e-10	n.a.
ρ (kg/m^3)	From Chemistry	1030	From material
C_p (J/kg/K)	From Chemistry	1050	From material
k_{eff} (W/m/K)	From Chemistry	0.209	From material

ε_{bed} = porosity of catalyst bed.
Θ_p = volume fraction of solid material in catalyst bed.
K = catalyst permeability.
n.a. = not applicable.

presented since the effect, on small variations of O_2, will be low for 600 ppm NO in the inlet. Essentially, no water (50 ppm) was present from the start of the experiments and none was added in order for us to be able to measure all gaseous components.

In order to be able to simulate the SCR reaction including the formation of by-products it is necessary to choose among our assumed reactions:

The reactions are demanding more and more oxygen and are being more important at increased temperatures the higher the number of the reaction is. The effect of diffusion limitations and the oxygen concentration is included in the rate constant obtained.

COMSOL Multiphysics ver. 5.2a was used in the simulations in a similar way as described before [21] with the data given in Table 3. Instead of the former used adiabatic conditions heat flux was used as the boundary condition on the outside of the reactor walls. The reactor was placed in a heated chamber with forced circulation of the air. Heat was transferred by convection from the reactor outside to the air flowing over sits outside according to: $q_0 = h*(T\_in-T)$. The value for h was 100 $W/m^2/K$ taken from [22] for forced convection, medium speed flow of air over a surface. The mesh size was calibrated for fluid dynamics and was of the size finer. The degrees of freedom (DOF = solved for was 76,983 plus 24,855 internal DOF for a first approximate solution). It was later needed to introduce 5 boundary layers close to the wall to get a fine resolution of the velocity profile in that position. Then the number of degrees of freedom was 134,018 plus 32,835 internal DOF.

The reactor is 465 mm long with the bottom of the catalyst bed positioned 108.3 mm from the inlet. Only a small part is shown (Fig. 2) in order to show the fine mesh used in the calculations. The catalyst bed, supported on quartz wool, is 8.3 mm long.

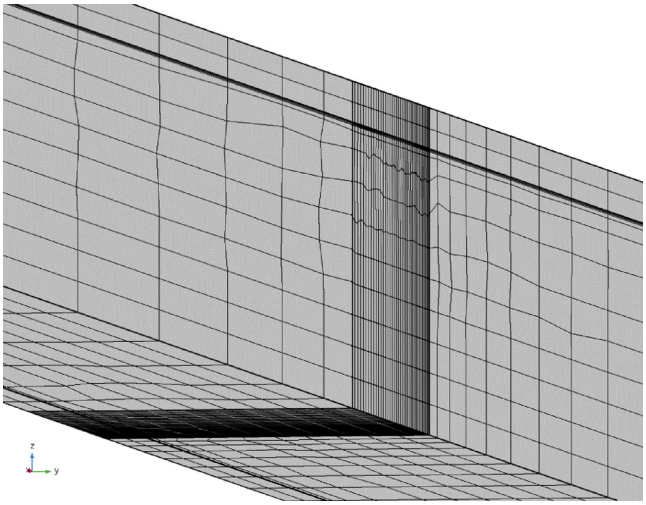

Fig. 2. Reactor model, showing the mesh, used in the simulations (1/8 of the whole cylinder). The gas inlet is from the right.

Table 4
BET surface area of catalysts before and after SCR test.

Catalyst sample	fresh	used	1*[a]	1*[b]	1*	2*	3*	5*	7*
before SCR	60.7	60.6	62.4	62.8	62.3	62.0	61.9	63.0	62.0
after SCR	64.0	58.9	63.5	62.0	62. 0	63.6	62.0	64.3	62.7

[a] Impregnated with unsaturated solution (0.12 g $CaSO_4$*2 H_2O per 500 ml water).
[b] Impregnated with unsaturated solution (0.53 g $CaSO_4$*2 H_2O per 500 ml water).

A thermocouple is positioned just after and in contact with the bed, measuring the outlet temperature. To avoid condensation of potential products, such as ammonium nitrate/nitrite, all sampling lines are insulated and heated to 195 °C.

Concentrations at the end of the reactor where simulations show that the concentrations are even over the channel cross section, are plotted versus the simulated temperature at the exit of the bed (108.3 mm). Manual changes in kinetic parameters are performed in order to fit the simulated values to the experimental ones according to the method described before [21].

3. Results and discussion

3.1. Surface area and pore structure of the catalyst samples

The values of the surface areas (mean 62.0 m^2/g before SCR and 62.6 m^2/g after SCR) are not varying much with the conditions (Table 4). There is no tendency that the surface area decreases after the SCR test. The catalyst is shown to be very temperature stable.

The values of the total pore volumes (the mean is 0.261 with a standard deviation of 0.007 cm^3/g before SCR and 0.256 and 0.012 cm^3/g after SCR) are not varying much with the conditions either. There is no tendency that the pore volume decreases after the SCR test. The catalyst pore system is shown not to be influenced by the impregnation.

After one impregnation, an amount of 0.16 mg deposited Ca (before SCR reaction bounded as $CaSO_4*2H_2O$, after SCR as a mixture of $CaSO_4*1/2H_2O$ and anhydrite) was supposed to be added in the pore system. Under idealistic conditions, the amount should have increased up to 1.12 mg (after seven times of impregnation with saturated $CaSO_4$ solution). 1.12 mg Ca corresponds to an amount of 4.81 mg $CaSO_4*2H_2O$ or 4.07 mg $CaSO_4$ (anhydrite) in the pore system, without considering the deposit of $CaSO_4$ on the catalyst outer surface and in the macropores. By using the density of $CaSO_4*2H_2O/CaSO_4$ (anhydrite), the calculated volume of the deposited material after one-time impregnation is 0.000286 cm^3. So, after seven times impregnation with a saturated $CaSO_4$ solution, one could expect a loss in pore volume of about 0.002 cm^3. This is only 0.8% of the average catalyst pore volume (0.26 cm^3). Thus, pore blocking and major changes in the pore system is not foreseen.

The average pore size before SCR is 167.5 ± 4.5 Å. After SCR it is 163.5 ± 5.7 Å. Thus it is not possible to say that the pore size distribution changes after the SCR reaction. It is also not dependant on the amount of Ca added.

Neither the surface area (within 1%) nor the total pore volume are changing with the impregnation process. There are also no changes after the SCR test showing that the catalyst used is very thermostable (Tables 5 and 6). This is to be expected since it was produces especially for the high temperature use in diesel applications.

3.2. Chemical analysis of the catalysts

SEM-EDAX and XPS were used to characterize the monolith form of

Table 5
XPS analysis of the fresh and the used catalysts.

Element	Fresh catalyst (wt %)	Used catalyst (wt %)	Assumedoxide	Calculated amount of oxide in the fresh catalyst (wt %)	Calculated amount of oxide in the used catalyst (wt %)
O	42.12	40.59			
Ca	0.00	1.07	CaO	0.00	1.69
C	8.81	9.11	C	0.00	0.00
Si	11.03	4.89	SiO_2	26.58	11.81
Al	3.30	1.67	Al_2O_3	7.02	3.56
P	0.00	0.07	P_2O_5	0.00	1.81
S	0.00	2.63	SO_4	0.00	8.90
V	0.55	0.24	V_2O_5	1.11	0.48
Ti	22.40	25.72	TiO_2	42.09	48.46
Mg	5.50	7.4	MgO	14.35	13.86
W	6.23	6.61	WO_3	8.85	9.41

Table 6
Conversion of NO for different samples. NO 600 ppm, NH_3 700 ppm, O_2 2%, 0.1 g catalyst, Flow 0.9 l_{NTP}/h, 3000 ppm Ar in Helium, p = 1.23 bar.

Catalyst	Conversion at 350 °C (%)	Optimal temperature (°C)	Conversion at the optimal temperature (%)	Content of Ca (mg/g)
fresh	64.3	425	88.00	n.d.
used	50.1	450	80.15	0.2244
1*[a]	28.4	500	65.15	0.2344
1*[b]	24.5	500	62.70	n.d.
1 *	24.3	500	63.68	0.2389
2 *	21.6	n.d.	n.d.	0.2523
3 *	16.5	500	52.07	0.2756
5 *	12.7	n.d.	n.d.	0.2904
7 *	11.0	525	44.83	0.2925

n.d.–value was not determined.
7* = impregnated 7 times with a saturated water solution of $CaSO_4$.
[a] Impregnated with unsaturated solution (0.12 g $CaSO_4$*2 H_2O per 500 ml water).
[b] Impregnated with unsaturated solution (0.53 g $CaSO_4$*2 H_2O per 500 ml water).

the fresh and the used catalysts. SEM analyses to a depth of around 1 μm while XPS only analyses the uppermost atom layers at the surface. Thus XPS is suitable for measuring the accumulation of small amounts of poisons on the surface. One should therefore suspect that the different methods give different results on the used catalyst. SEM was used to determine the contents of W, Si, Ca, V and Ti over the used catalyst wall (details not shown here). The following results were obtained (mean wt% as oxides): 0.42% V_2O_5, 7.1% WO_3 on 88.3% TiO_2 containing 3.8% SiO_2 and 0.41% CaO. The main catalyst components V, W and Ti vary over the cross section within 10% of their respective mean values. Silica varies as much as 1.8 wt% because at certain positions a silica fibre is located. Ca also varies with 1 wt%. The content of Ca is generally low except at certain points in the catalyst. This could be an indication that the Ca preferably deposits at the outer surface of the catalyst when used in the diesel engine. It can be assumed that the catalyst is a low vanadia content catalyst (0.48 wt% according to XPS (Table 5) and 0.42 according to SEM). The value from SEM are representative for the inner parts of the catalyst since they were measured over the wall cross section of 0.14 mm. Fifteen (15) different places over the catalyst wall cross section were measured and the scatter in data are small for the active components.

Table 5 gives the result from the XPS analysis. We have recalculated the amount of various compounds as the oxides given in the Table. No Ca, P or S was detected in the fresh catalyst.

The molar amounts shown below are moles per 100 g of catalyst. There is a lot of Mg in the fresh catalyst and much of the Mg is probably present as a binder as a $Mg(AlSiO_4)_2$ glass (0.1223 mol) in the fresh catalyst. Aluminium is the limiting component for the glass in the fresh catalyst. Other compounds, except for the active SCR catalyst ingredients, are 0.165 mol MgO and 0.332 mol SiO_2 in the form of silica fibre glass.

The used catalyst contains 1.7% Ca, 0.07% P and 2.63% SO_4. Some of the probable compounds are; $CaSO_4$ (0.0267 mol), $Mg(AlSiO_4)_2$ (0.0310 mol), $MgSO_4$ (0.0536 mol), $MgHPO_4$ (0.0027 mol) and MgO (0.2182 mol). It is demonstrated that there are large amounts of SiO_2 (probably as reinforcement silica fibres) in the fresh and the used catalysts.

The content of the support is 42.1 wt% TiO_2 in the fresh catalyst and 48.5% in the used one. WO_3 is around 8.9 wt% in the fresh catalyst and 9.4% in the used one.

The analysis by XPS is very sensitive to the composition on the precise location for the measurements. These measurements never arrive at the right content of TiO_2 (probably 88% s in the used by SEM above). Instead we arrive at 42–48 %. The amount of WO_3 by XPS is 8–9% instead as 7% by SEM. V_2O_5 is 1.1% in the fresh catalyst and 0.48% in the used one (0.42% by SEM).

Gao et al. [23] prepared a similar catalyst with V:W:Mo:TiO_2:fibre glass = 1:4.5:4.5:72:18. The difference is that Mo is not present in our catalyst and is replaced by W. Alemany et al. [24] characterized V_2O_5-WO_3/TiO_2 de-NO_x catalysts with 9% WO_3 and 1% V_2O_5, similar to ours. The surface areas are higher (87 m^2/g) but the pore volume 0.30 close to ours at 0.26 cm^3/g.

Components from the lubricant oil for the engine are present as 0.07 wt% P in the used catalyst. The lubricating oil usually also contains Zn but no Zn could be detected. Ca is present at 1.07 and S at 2.63 wt%. Some of the Ca, S and Mg could well come from the lubrication oil [14]. The presence of even higher Ca amounts (1.79 wt%) was observed by Schobing et al. [25].

Shen et al. [26] presented a XPS analysis with the following contents V 1.12, W 5.75 and Ti 27.36 wt%. These values are very close to ours except for that our catalyst contained a lower amount of vanadium.

3.3. TPD of ammonia

From the analysis of the shape of the TPD curve it can be concluded that the ammonia adsorption does not take place only on a single site or that the adsorption energy varies with coverage. During the TPD, N_2 was desorbed. However, the amount of N_2 was approximately 0.2% of the desorbed amount of NH_3, so the contribution of the reaction of ammonia to nitrogen was small in our SCR model. To avoid introducing more than one site into the model it was assumed that the activation energy for desorption was a function of the surface coverage [27]:

$$\Delta H_{NH3} = \Delta H_{NH30}{}^{*}(1 + \alpha{}^{*}\theta_{NH3}{}^{\beta})$$

The result from the TPD (not shown here) is a value of ΔH_{NH30} of −240 kJ/mol, $\alpha = -0.44$ and $\beta = 0.36$.

The values of theses constants must be adjusted in the simulations.

3.4. Activity of the catalyst samples

Fig. 3 shows the experimental data for the NO content at the reactor exit as a function of temperature. The fresh and the used catalysts have minima in the NO content at 425 and 450 °C. Then the concentration increases again. This can be the effect of ammonia desorbing at high temperatures making the SCR reaction slower. It could also be an effect of NH3 being oxidized to NO. The effect of temperature is large and the conversion of NO is 80% at its maximum and decreases to 58% at 550 °C. Similar effects are not seen for the impregnated catalysts (1* and 7*). The poisoning causes the concentration of NO to approach a constant value at high temperatures. This can be an effect of lowering

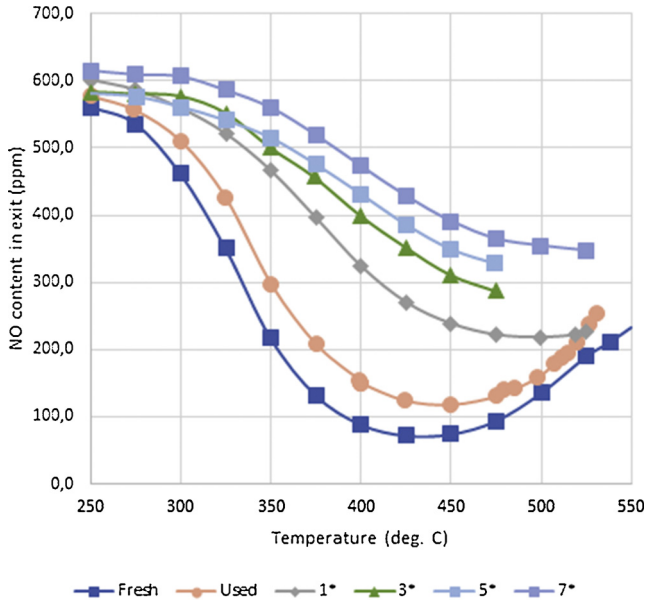

Fig. 3. Experimental data of outlet ppm values for NO for all catalyst samples used in the simulations. Inlet conditions 604 ± 12 ppm NO, 649 ± 12 ppm NH_3, 2% O_2 and 1.236 ± 0.011 bar.

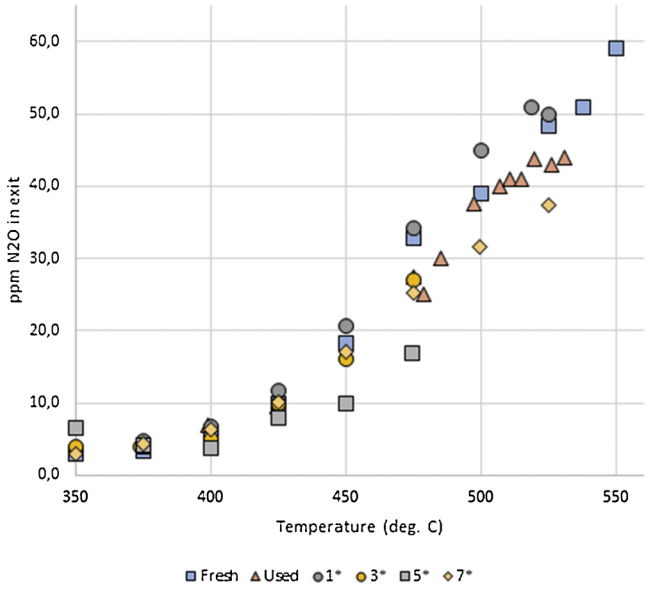

Fig. 4. Experimental data of outlet ppm values for N_2O for all catalyst samples used in the simulations. Inlet conditions 604 ± 12 ppm NO, 649 ± 12 ppm NH_3, 2% O_2 and 1.236 ± 0.011 bar.

the heat of adsorption of ammonia (ΔH_{NH3}) and thus of decreasing values of the adsorption constant (K_{NH3}). It is also clear from the Figure that the activity decreases for more poisoned catalysts. Only the data from the fresh, used, 1* and 7* samples were used in the simulations.

Fig. 4 shows the content of N_2O in the exit of the reactor. At temperatures up to 400 °C they follow each other closely. The material that gives the smallest amount of N_2O at 525 °C is the 7 times impregnated one (37 ppm). The fresh gives 49 ppm, the used gives 43 ppm and the 1 time impregnated 50 ppm N_2O.

There is a clear trend of decreasing conversion of NO with increased amount of Ca (Table 6). The conversion at 350 °C (Table 6) decreases from 64.3% for the fresh catalyst down to 50.1% for the used one (a decrease by 22%). Despite the high Ca content of the used catalyst (0.2244 mg Ca/g catalyst) its effect on activity is not very large. The

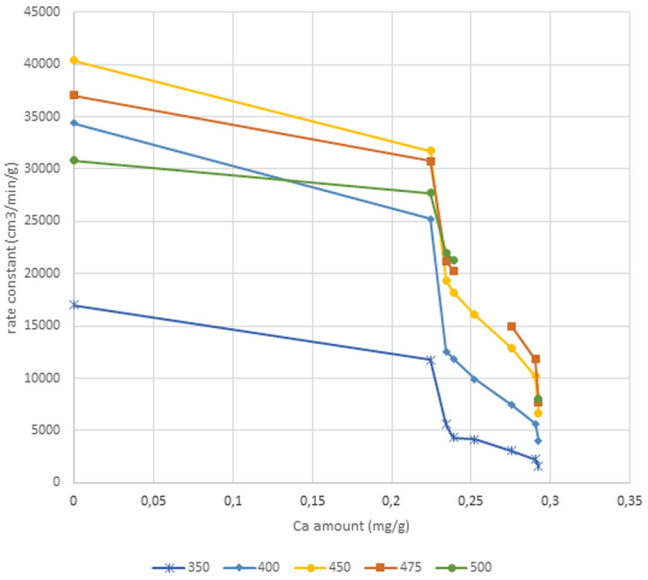

Fig. 5. Effect of amount of Ca on the rate constant at 350, 400, 450, 475 and 500 °C. Inlet values of NO are around 608 ppm, NH_3 around 655 ppm, O2 2%, 3000 ppm Ar in helium. 0.1 g catalyst, 900 cm^3NTP/min total flow, 1.25 bar.

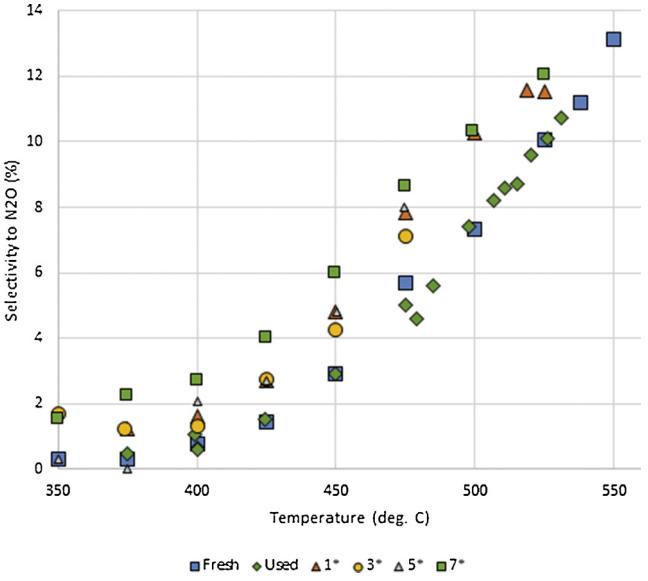

Fig. 6. Selectivity to formation of N_2O as a function of the reaction temperature for catalysts used in the simulations. Inlet conditions 604 ± 12 ppm NO, 649 ± 12 ppm NH_3, 2% O_2 and 1.236 ± 0.011 bar.

conversion for the 7 times impregnated catalyst is only 11%.

There is also an increase in the optimal temperature for conversion of NO from 425 °C for the fresh catalyst to 500–525 °C for impregnated catalysts. Our values compare nicely with the ones of Koebel and Elsener [28]. They obtained a conversion of 1020 ppm NO to 87% at 400 °C, which is in between our values for the fresh catalyst of 64.3% at 350 °C and 88.0% at 425 °C.

The rate constants (calculated from the data in Fig. 3 and other experimental data) vary with the amount of Ca in the catalysts. The fresh catalyst does not to contain any Ca (Table 5). The used one contains a considerable amount (0.244 mg/g catalyst). The values of k/k_{fresh} for the used one were 0.567, 0.676 and 0.718 at 300, 350 and 400 °C. Thus, the relative rate of deactivation was largest at the lowest temperatures. For the catalyst impregnated 7 times the corresponding values were 0.134, 0.113 and 0.149. The largest decrease in activity in this case is at 350 °C. There is a maximum in the rate constant for the

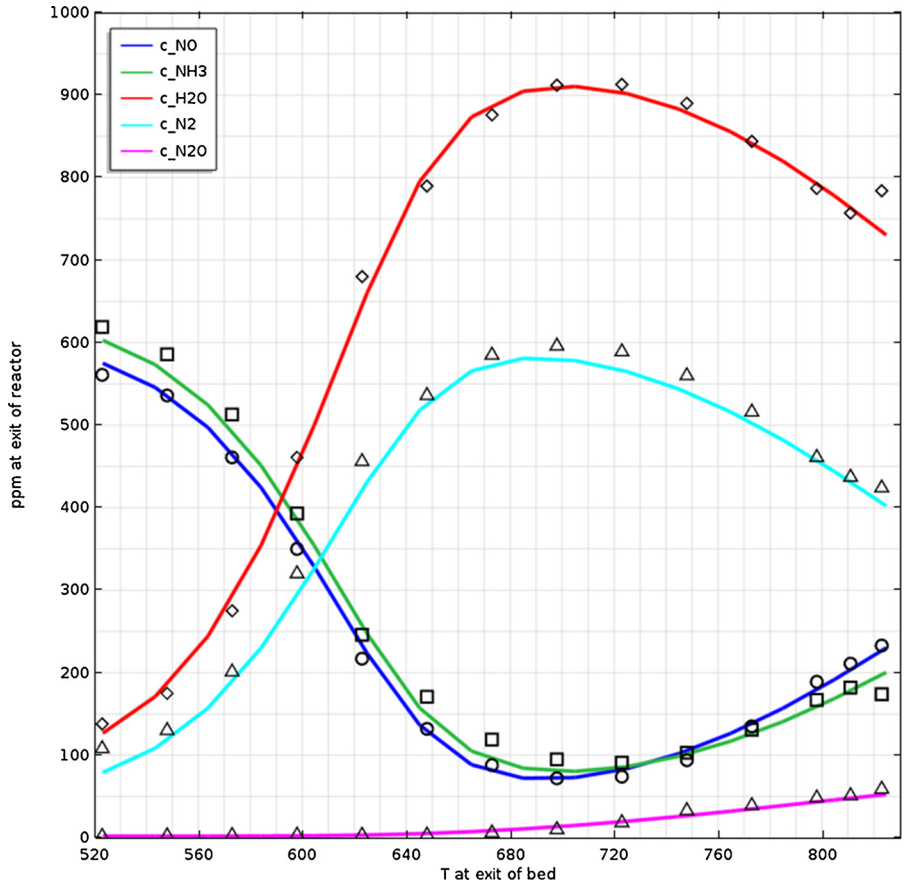

Fig. 7. Comparison of simulated concentrations to experimental values for all components for the fresh catalyst. Experimental values in ppm; circles NO, squares NH_3, diamonds H_2O, upper triangles N_2 and bottom triangles N_2O. Lines are simulated values.

fresh catalyst at 450 °C. When the used catalyst is impregnated once with saturated $CaSO_4$, there is a large drop in rate constant, higher at higher temperatures (Fig. 5). Most of the amount of Ca in the used catalysts probably comes from the lubricating oil and from the water used for the urea solution and is deposited as $CaSO_4$ on the outside of the catalyst monoliths. Thus, the Ca added by impregnation introduces a stronger deactivating effect on the catalyst than that present in the used catalyst because it is evenly distributed in the catalyst pore system. Thus, the influences of different forms of Ca in the catalyst are of different kinds. Because of the use of Ca in the form of sulphate in the impregnation, and its low water solubility, very small amounts have been introduced. From Fig. 5 one can extrapolated that, at 400 °C, the catalyst will be totally deactivated at an amount of Ca of 0.29 mg/g. The figures are not much different at 350 and 300 °C.

The rate constants vary with temperature according to an Arrhenius expression. Koebel and Elsener [28] report rate constants which are in the same range as ours at 400 °C and an effectiveness factor of 0.57. Tang et al. [29] studied the deactivation of an in house made V_2O_5/TiO_2 catalyst containing 3.87 wt% V_2O_5 with Na and Ca from nitrates. The fresh catalyst's conversion at 310 °C was 0.441. After an addition of Ca/V of 0.02 the conversion was 0.434, a very slight deactivation. At Ca/V = 0.2 the conversion dropped to 0.242. The drop in conversion was linear in the Ca content as we also observed. Our values of the Ca/V calculated from the added amount of Ca were much lower (0.00053–0.00361) so again the deactivation presented here is very strong. Tang et al. [29] observed that at Ca/V = 0.20 the rate constant was $2.78*10^3$ $cm^3/g/min$ and 310 °C. Their fresh catalyst had a rate constant of $5.83*10^3$ $cm^3/g/min$, thus the decrease was 52.3%. This decrease is about the same as ours, but our Ca contents are much lower. They also observed that the amount of weak acid sites increases for a Ca-poisoned catalyst while the total amount remains independent on the amount of Ca (i.e. the amount of the strong sites decreases).

The apparent experimentally determined activation energies (temperature range 275–350 °C) vary with the sample. The fresh catalyst has an apparent activation energy of 80 kJ/mol and the used catalyst has an apparent activation energy of 88 kJ/mol. The values for the impregnated catalysts were: 1* 90 kJ/mol, 2* 95 kJ/mol, 3* 63 kJ/mol, 5* 66 kJ/mol and 7* 51 kJ/mol. The more poisoned catalysts have lower activation energies as we have shown before [30].

In an experimental study on the kinetics of NO reduction on commercial de-NO_x catalysts Koebel and Elsener [28] obtained Ea values in the range 73–86 kJ/mol for fresh catalysts. Their values are in the same range as ours but are corrected for diffusion influence. Koebel and Elsener also found that the value for the apparent Ea was dependent of the amount of NO present. The value given for catalyst D21 was 83 kJ/mol for 1000 pm inlet NO. For an inlet content of 250 ppm NO the value was 75 kJ/mol and for 70 ppm NO the value was 70 kJ/mol. A similar trend was obtained for two other catalysts.

Kröcher and Elsener [14] show that the effect of $CaSO_4$ (impregnated with Ca acetate and treated with SO_2 at 400 °C for 5 h for formation of the sulphate) should be slight while the effect of Ca (acetate) should be medium to strong. These results seem similar to ours. Chen and co-workers [31] studied a, in house prepared, 5 wt% V_2O_5/TiO_2 catalyst impregnated with Ca acetate. For a particle size of 0.694 mm and at Ca/V = 0.02 the effect of Ca was a decrease in rate constant by 18%. This is still a much higher value of Ca/V than presented here. Their values of the rate constant for the fresh catalyst was $0.63*10^3$ $cm^3/g/min$ while ours was $4.34*10^3$ $cm^3/g/min$.

Since the SCR reaction is very fast internal diffusion limitations are foreseen. The calculated effectiveness factor (η) for the fresh catalyst

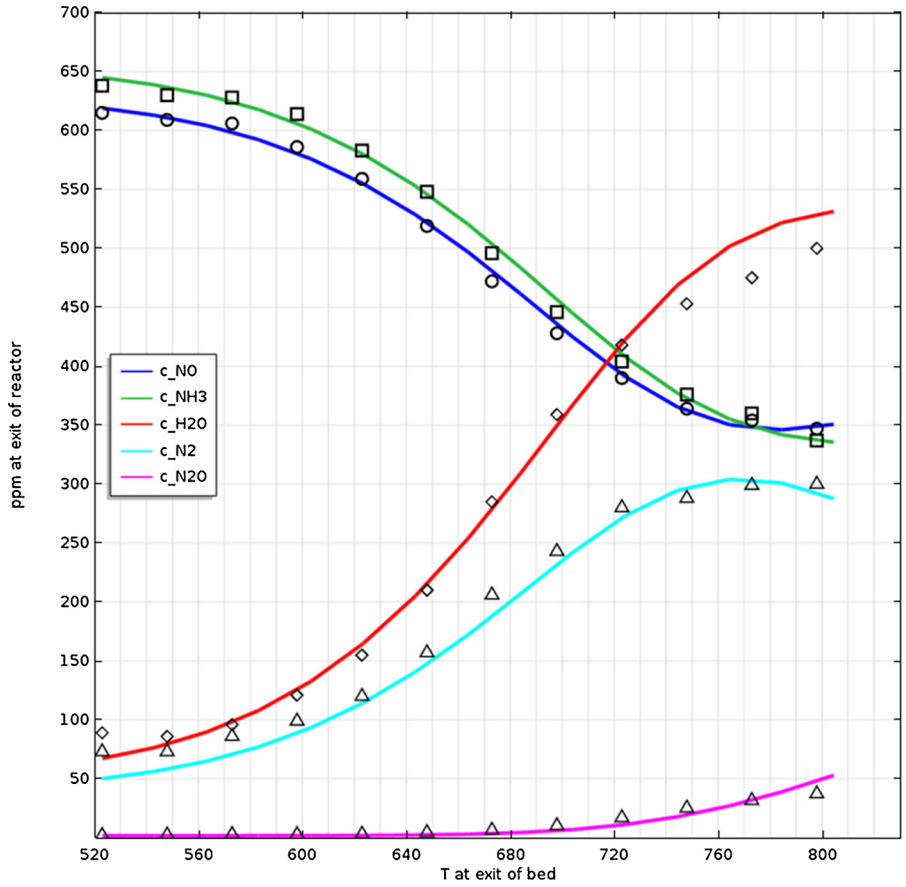

Fig. 8. Comparison of simulated concentrations to experimental values for all components for the catalyst impregnated 7 times. Experimental values in ppm; circles NO, squares NH_3, diamonds H_2O, upper triangles N_2 and bottom triangles N_2O. Lines are simulated values.

(d_p = 0.6125 mm) is 0.7 at 250 °C and there are no external limitations for mass or temperature as calculated by methods given by Mears [32,33,34]. The reaction is limited by pore diffusion though, but the whole catalyst is used for the reaction. The intrinsic 1st order rate constant is $1.65*10^3$ cm^3/g/min. The main other gradient is along the axis of the reactor. A temperature increase of 3 °C is calculated along the catalyst bed.

At 400 °C, the calculated effectiveness factor is 0.057 and the reaction is strongly limited by pore diffusion and only the outmost 20% of the catalyst particle is used in the reaction. The intrinsic rate constant is $6.54*10^5$ cm^3/g/min. These two intrinsic rate constants result in an intrinsic activation energy of 116.7 kJ/mol. In this case, the temperature increase along the reactor axis is calculated by Mears method to 32 °C. At 400 °C, Koebel [28] report that the η is 0.57 at 400 °C for particles of 160–200 μm diameter. Ours had an average diameter of 612.5 μm. This is the reason for the much lower value of η in our experiments.

The effect of the dissolved Ca^{2+} introduced to the used catalyst is probably to coordinate to two V−OH groups. By this process the adsorption of ammonia on these Brønsted acid sites is hindered and thereby the activity is lowered. The SO_4^{2-} ions are coordinated to the TiO_2 support generating new acidic sites. The deactivation by Ca is dominating. In fact Nicosia et al. [15] showed by DFT calculations that one atom of Ca deactivates 4 atoms of V. This could be the reason for the strong deactivation observed.

3.5. Selectivity to formation of N_2O

The selectivity to formation of N_2O is dependent on the poisoning by Ca as shown in Fig. 6. The fresh and the on the engine used catalyst show similar trends with increasing selectivities from around 0.5% at 350 °C to 11% at 538 °C. This is in line with that the Ca has not penetrated much into the pores of the catalyst and thus not influenced the selectivity in comparison to the fresh catalyst. With increased amount of Ca (1*) the selectivity to N_2O increases to 1.2% at 375 °C and 11.5% at 525 °C. Even higher Ca amounts (7*) gives 1.5% at 350 °C and 12% at 525 °C. Thus the effects are largest at lower temperatures and the selectivities approach each other at high temperatures.

This can be compared to data from Djerad et al. [35]. They studied the effect of oxygen on the formation of N_2O over a similar catalyst to ours. From 500 ppm NO and 500 ppm NH_3 the N_2O formed was 210 ppm at 500 °C and 2% O_2. We obtained 40 ppm. The difference is caused by the 3% V_2O_5 in their catalyst causing the larger amounts of N_2O. They also reported that increasing the O_2 content to 15 vol.% decreased the formation of N_2O to 150 ppm. Lietti et al. [36] found selectivities for commercial V_2O_5 (0.8%)-WO_3 (9%)/TiO_2 catalysts of 2.6% at 352 °C and 11.37% at 477 °C under dry conditions. These are in the same range as ours especially considering that higher selectivities for N_2O are expected at higher contents of V_2O_5 [37]. Duffy et al. [38] studied the formation of N_2O on vanadia-titania catalysts from 200 to 500 °C using ^{15}NO and $^{14}NH_3$. Below 350 °C only $^{14}N^{15}N$ is formed meaning that NO and NH_3 contributes equally to the formation of N_2. At higher temperatures the products formed are dependent on the amount of V_2O_5 in the catalyst. This is in agreement with results from our earlier work [39]. Ammonia oxidation to ^{14}NO takes dominates at 500 °C over a 100% V_2O_5 catalyst. The 1.4% one produces less $^{14}N^{15}NO$ than the ones with higher contents of V_2O_5. At 400 °C the ammonia oxidation to ^{14}NO is causing the decrease in the conversion of NO as seen above for the fresh and the used catalyst.

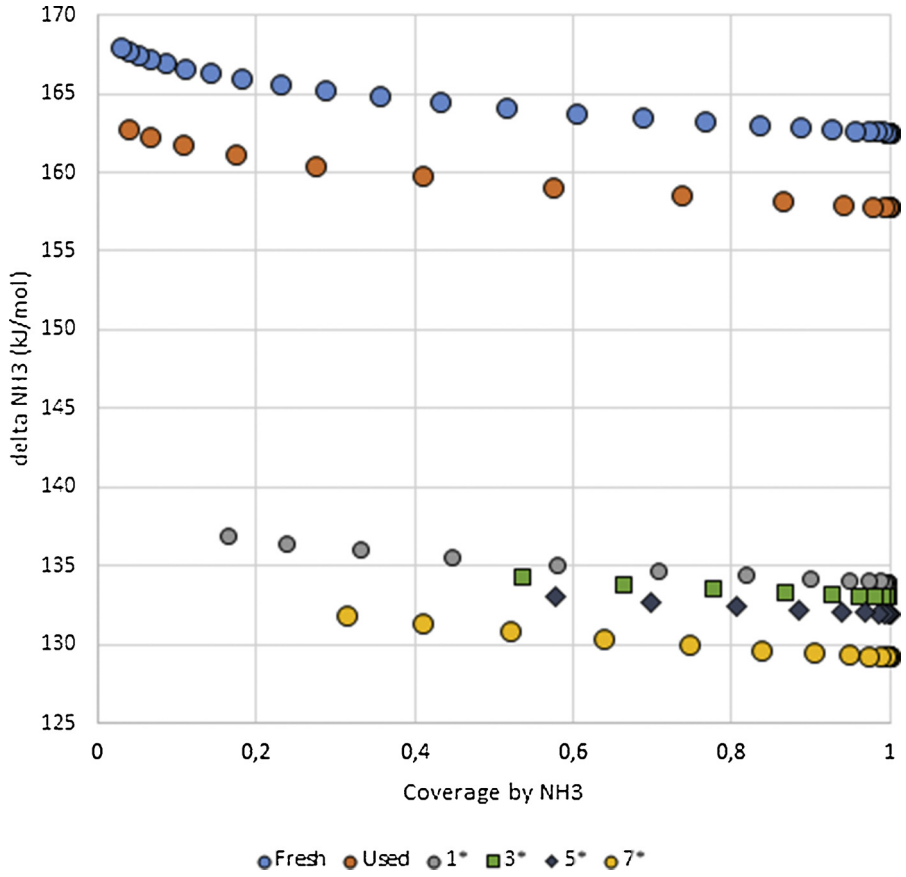

Fig. 9. The effect of ammonia coverage on the heat of adsorption of ammonia from simulations. Inlet conditions 604 ± 12 ppm NO, 649 ± 12 ppm NH_3, 2% O_2 and 1.236 ± 0.011 bar.

Table 7
Kinetic data for the model obtained in the simulations.

Parameter	Catalyst					
	Fresh	Used	1*	3*	5*	7*
K_{NH30} (m^3/mol)	$1.04*10^{-10}$	$1.86*10^{-10}$	$6.08*10^{-8}$	$4.95*10^{-8}$	$9.1*10^{-8}$	$1.87*10^{-7}$
Δ_{NH30} (kJ/mol)	−170	−165	−140	−139	−138	−137
α	−0.044	−0.044	−0.044	−0.044	−0.044	−0.044
β	0.36	0.36	0.36	0.36	0.36	0.36
A_1 (1/s)	$6.70*10^{7}$	$2.00*10^{8}$	$1.69*10^{6}$	$1.21*10^{6}$	$2.41*10^{5}$	$1.25*10^{5}$
E_1 (kJ/mol)	82	90	70	70	63	65
A_2 (mol/m^3/s)	$3.75*10^{3}$	$1.50*10^{3}$	300	$1.65*10^{3}$	840	60
E_2 (kJ/mol)	80	75	70	75	75	65
A_3 (1/s)	$8.88*10^{10}$	$6.48*10^{10}$	$2.07*10^{10}$	$2.59*10^{10}$	$2.35*10^{10}$	$1.18*10^{10}$
E_3 (kJ/mol)	150	150	150	150	150	150
A_4 (mol/m^3/s)	$2.56*10^{10}$	$3.49*10^{10}$	$6.20*10^{9}$	$7.75*10^{9}$	$7.75*10^{9}$	$2.08*10^{9}$
E_4 (kJ/mol)	170	170	170	170	170	170

3.6. Simulation of catalyst behaviour

The model describes the experimental data very well (Figs. 7 and 8). The only data that were fitted are the concentrations of NO and N_2O. Even so the simulated values of all other products H_2O and N_2 as well as the reactant NH_3 are nicely predicted except at the very highest temperatures. This result could only be obtained using simulation with a program, which considers many different physics. The most important factor is the temperature rise in the catalyst bed, which will be described below.

In the model used the adsorption constant for NH_3 is given below:

$$K_{NH3} = K_{NH30}*\exp(-\Delta_{NH3}/(R*T))$$

$$\Delta H_{NH3} = \Delta H_{NH30}*(1 + \alpha*\theta_{NH3}\hat{}\beta)$$

$$\theta_{NH3} = K_{NH3}*c_{NH3}/(1 + K_{NH3}*c_{NH3})$$

As shown in Fig. 9 the value of the heat of adsorption of NH_3 varies considerably with the coverage by NH_3 as a result of fitting the kinetics on different catalysts. This causes the adsorption constant to vary with temperature and catalyst. The values of the K_{NH30} are given in Table 7. The highest value is obtained for the fresh catalyst ($\Delta H_{NH3} = -170$ kJ/mol). The value for the used catalyst is only a little lower ($\Delta H_{NH3} = -165$ kJ/mol). The value decrease to −140 and −137 kJ/mol for the 1* and 7* impregnated catalysts. This is in line with theory which supposed that the acid sites with the highest strength are the ones poisoned first.

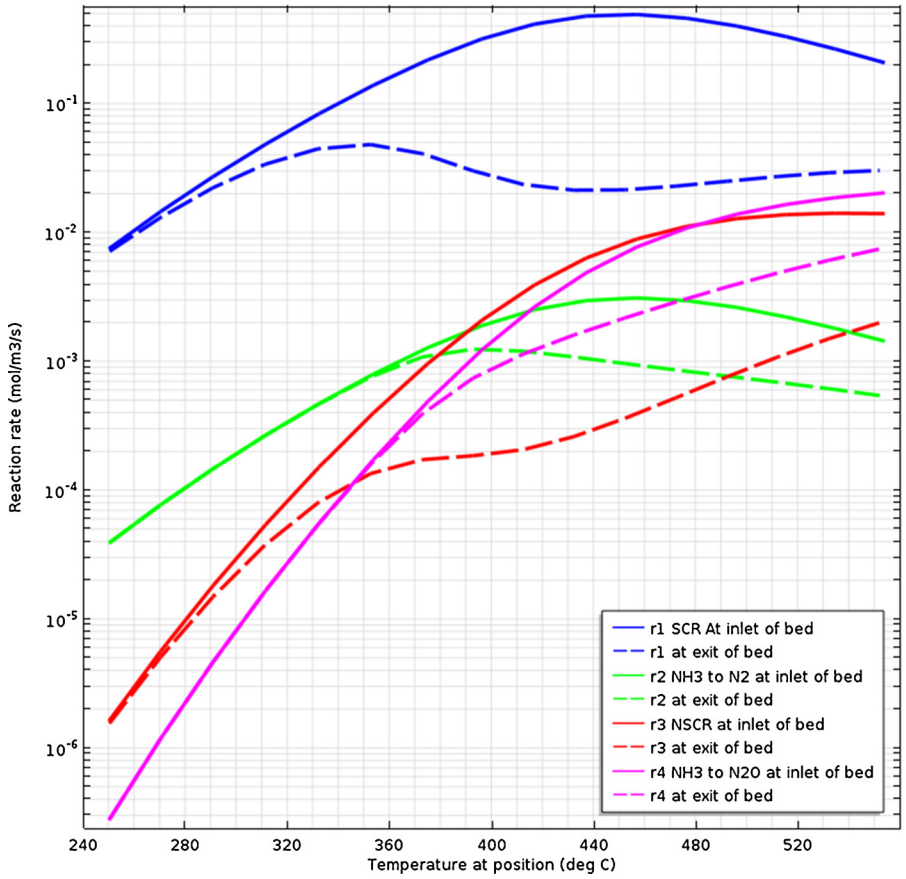

Fig. 10. Rates as a function of the temperature for the four reactions in the simulation of the fresh catalyst.

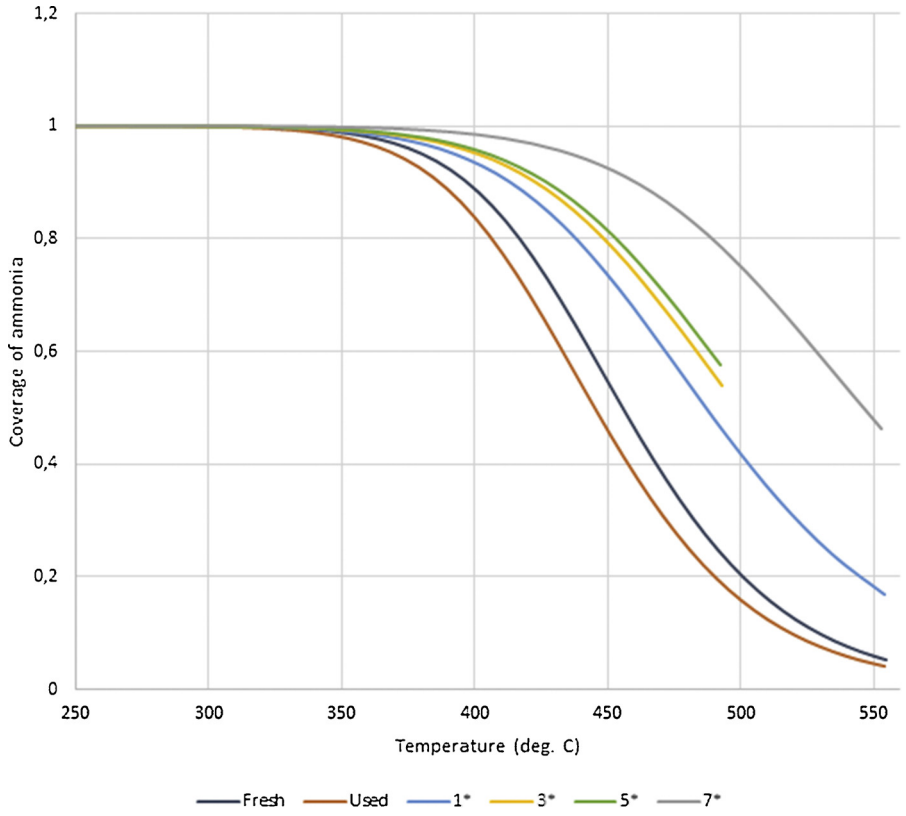

Fig. 11. The simulated coverage of ammonia for all catalysts as a function of the temperature. Inlet conditions 604 ± 12 ppm NO, 649 ± 12 ppm NH_3, 2% O_2 and 1.236 ± 0.011 bar.

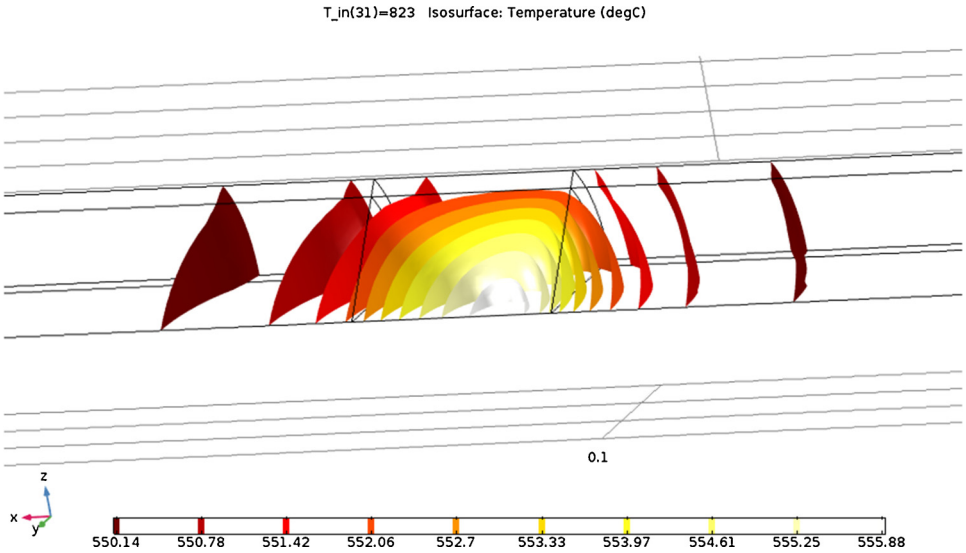

Fig. 12. Simulated temperature development in the reactor at an inlet temperature of 550 °C. The gas inlet comes from the right in the Figure. Fresh catalyst. 608 ppm NO, 636 ppm NH_3, 2% O_2, 1.26 bar. Isothermal contours.

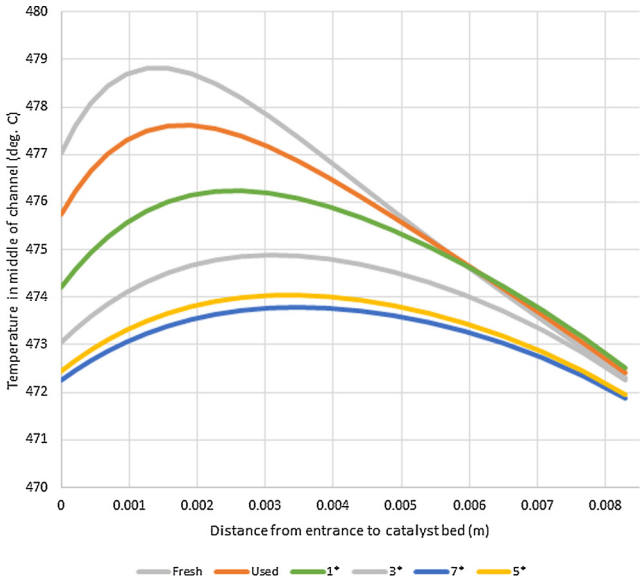

Fig. 13. Simulated temperature profiles along the catalyst bed axis for an inlet temperature of 470 °C for simulated catalysts. Inlet conditions 604 ± 12 ppm NO, 649 ± 12 ppm NH_3, 2% O_2 and 1.236 ± 0.011 bar.

It was not necessary to take all assumed reactions in Table 2 into consideration. Only reactions 1–4 were the ones necessary to represent the system and only the SCR reaction (1) is fast enough to be influenced by pore diffusion limitation (Fig. 10). Thus, its apparent activation energy (E_1) varies for different samples along with the varying activity. Both reactions yielding N_2O, the low temperature non selective reduction (NSCR) of NO by NH_3 (3) and the direct oxidation of NH_3 to N_2O (4), which dominates at high temperatures, have constant activation energies (E_3 and E_4 respectively). The value of A_1 varies a lot from $4.47*10^7$ for the fresh sample to $5*10^4$ for the most deactivated one. Thus, it decreases by 99.9%.

A very strong deactivation is thus observed considering the small amount of Ca introduced. Koebel and Elsener [28] found an adsorption energy for ammonia on the catalyst of −137 kJ/mol which in the region of our values. Roduit et al. [20] determined K_{NH30} to $*10^{-8}$ in our units and the heat of adsorption of NH_3 to 139 kJ/mol. These values are close to ours in Table 7 for the 1* and the 7* impregnated catalysts. Xiong et al. [40] proposed a global reaction scheme similar to ours including a reaction mechanism. They included the NSCR, yielding N_2O, above 300 °C and the oxidation of NH_3 to NO at 350 °C and above. It was not necessary for us to include this latter reaction.

The value of the coverage by NH_3 (Fig. 11) has a large effect on the simulations at temperatures when the value of the coverage becomes much smaller than 1, i.e. above around 400 °C. This is because the coverage by ammonia is included in all reaction rate expressions used in the simulations. It was necessary to change parameters affecting the coverage after first fitting the data at lower temperatures where the SCR reaction dominates and where the coverage is 1. Roduit et al. [20] shows that the coverage by NH_3 at 650 ppm NH_3 is less than 1 at 400 °C. We observe (Fig. 11) a rapid decrease in the ammonia coverage above 400 °C. The decrease is less rapid for the deactivated catalysts.

It is clear from Fig. 12 that a temperature increase of 6 °C is obtained because of the heat developed in the reactions at an inlet temperature of 550 °C. The heat is produced by the reactions in the short (0.83 cm) catalyst layer. Because of the heat exchange to the flowing air, in the oven, which regulates the reactor temperature, there is only a short region around the catalyst bed, which has an increased temperature. The maximal temperature inside the bed is 556 °C in a small region in the centre of the bed and after about one fourth of its length (Fig. 13).

The maximal temperature (478.8 °C) is reached only 1.4 mm from the inlet of the bed for the fresh catalyst and somewhat longer into the bed for the used catalyst (Fig. 14) at an inlet temperature of 470 °C where the rate of the SCR reaction is at its maximum. It is therefore important to use a tight mesh in the calculations in the bed and a distribution with many nodes (in all 40 nodes) close to the inlet as we did. The value of the temperature at its maximum decreases along with the poisoning of the catalyst. For the most poisoned one (7*) the maximal temperature is 473.8 °C at 3.5 mm from the inlet of the catalyst bed. It is also demonstrated that at the inlet of the bed an increase of the temperature by 7 °C is obtained for the fresh catalyst. Nowhere inside the bed the temperature is lower than 471.9 °C. Heat is transported through conduction in the wall and heats the inlet gas. Thus, the temperature effect goes outside of the catalyst bed. Thus, these temperature effects will change the concentration of the species in the inlet of the bed and thus influence the rate of reactions. The more poisoned materials have maxima further inside the catalyst layer (2.5 mm for 1* impregnated and 3.5 mm for the 7* impregnated) as can be expected for less active catalysts. The temperature effects are so large that non-isothermal conditions prevail and isothermal evaluation of the kinetics will be difficult. This demonstrates that the method used here gives valuable results.

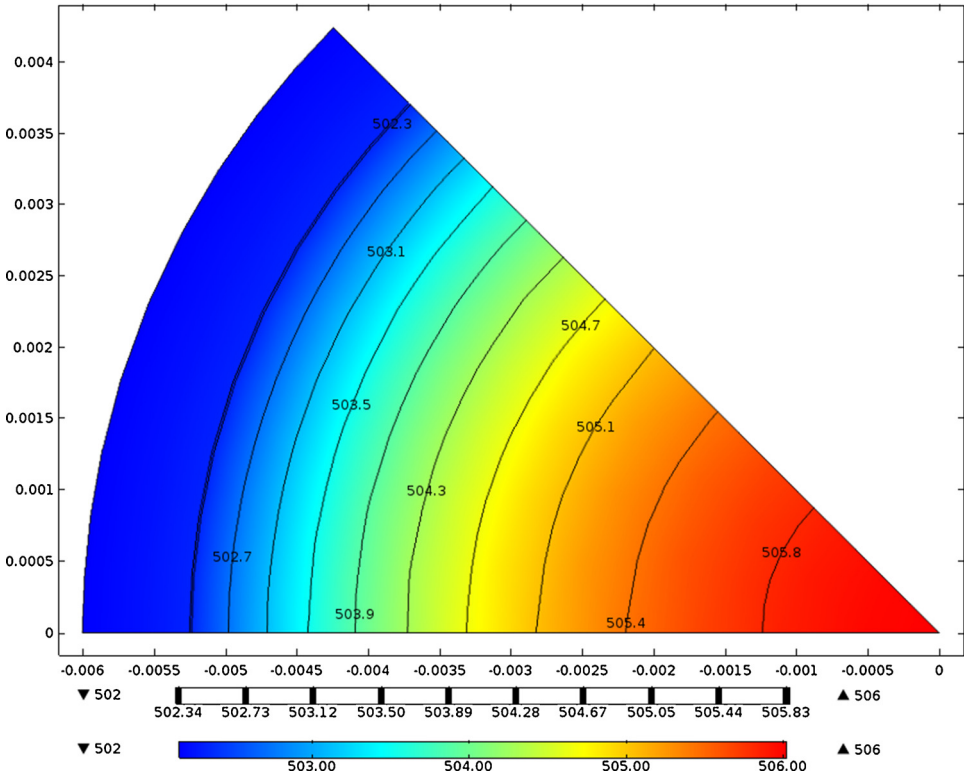

Fig. 14. Simulated temperature distribution over the cross section of the exit of the fresh catalyst bed at an inlet temperature of 500 °C.

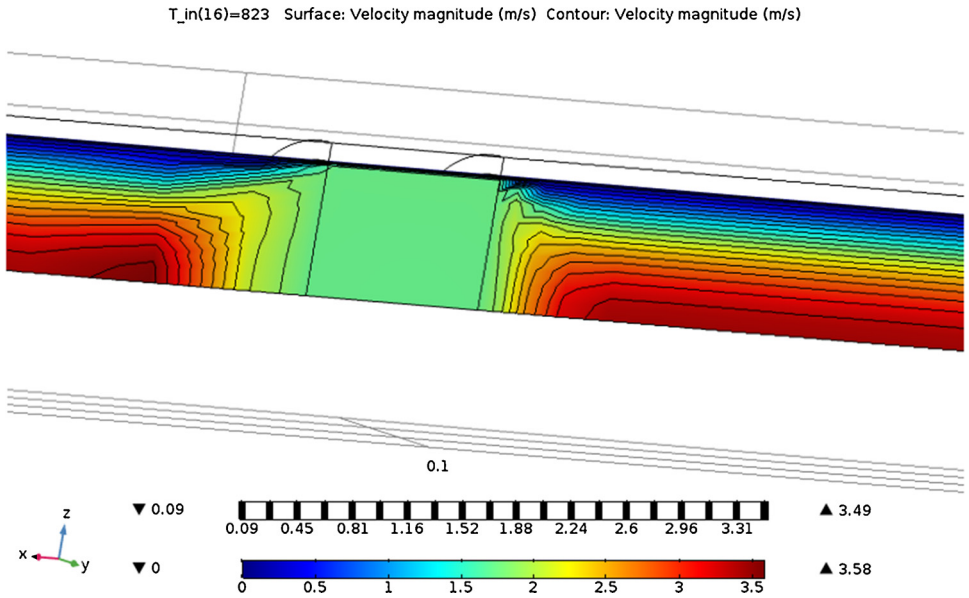

Fig. 15. The velocity distribution in and around the catalyst bed at an inlet temperature of 550 °C. Used catalyst. Inlet conditions 597 ppm NO, 629 ppm NH_3, 2% O_2 and 1.23 bar.

Mears [32,33,34] do not take the cooling from the outside of the reactor into consideration in the method. That is why our temperature increase is lower than the 32 °C predicted above.

Fig. 14 shows the temperature distribution over the catalyst bed cross section at its exit. In the centre, where the thermocouple is located, the highest temperature is reached. It is 506 °C whereas it is only 502.3 °C close to the wall (when the contour is divided in 10 sections). The temperature in the wall is 502 °C.

The conversion of NO increases in a regular fashion with the distance from the inlet of the bed. The exit value is 0.655 for the fresh and 0.635 for the used catalyst at the exit. Lower conversions are simulated for the poisoned ones (0.578 for 1* and 0.423 for 7 * impregnated catalysts).

The catalyst bed is so compact that most of the bed experiences the same velocity of around 1.59 m/s (Fig. 15). There is a small section close to the wall with very low velocity as expected. In this simulation, the number of boundary layers is 3. No boundary layers were used in most of the simulations since their introduction increases the time considerably. In addition, they were not needed in order to get the right concentrations. They do influence the thickness of the boundary layer

at the wall considerably. This even velocity in the bed yields excellent conditions for equal rates across the radius in the whole bed. In this way, the catalyst is used most effectively for chemical reactions. On both sides of the bed there is rapidly developing a velocity profile over the reactor cross section. Outside the bed, the velocity is largest in the centre and approaches 0 at the wall as expected.

4. Conclusions

The deactivation of the SCR catalyst is not connected to a loss of BET-surface area or changes in the pore structure; it is a chemical phenomenon. It is clear that Ca introduced into the pore system by impregnation poisons the catalyst strongly and in a different way from when it is coming from the engine during operation. There is an almost linear decrease in the rate constant with the amount of Ca impregnated on to the used catalyst. The effect of deactivation is largest at lower temperatures. The rate constant for the fresh catalyst at 400 °C was $3.44*10^4$ cm^3/min/g. After 2729 h deactivation in the diesel plant (used catalyst) it was $2.52*10^4$ cm^3/min/g (−26.7%). After impregnation of the used catalyst once with a saturated solution of $CaSO_4$ the value of the rate constant was $1.14*10^4$ cm^3/min/g (−66.9%) and after 7 times it was $4.02*10^3$ cm^3/min/g (−88.3%). The apparent experimental activation energies decreased with the degree of poisoning down to 51 kJ/mol for the 7* impregnated sample.

This is, to our knowledge, the first time data on the simulation of the SCR reaction for Ca poisoned catalysts is presented. The model used describes the concentrations of all components in the SCR reactions, NO, NH_3, H_2O, N_2 and N_2O in a surprisingly fine way. This is true for all the catalysts studied. The activities are well represented by the changes in the pre-exponential factors and activation energies presented in Table 7. By using the proposed model with three reactions and only fitting the concentrations of NO and N_2O both NH_3 and the products N_2 and H_2O are nicely represented.

Acknowledgements

We wish to thank Mr Christoph Becker who performed the reaction experiments. Mrs Birgitta Lindén helped us with the nitrogen adsorption measurements. A Swedish diesel power plant is acknowledged for supplying the used catalyst. This research did not receive any specific grants from funding agencies in the public, commercial, or not-for-profit sectors.

References

[1] A. Konstandopoulos, D. Zarvalis, L. Chasapidis, L. Deloglou, N. Vlachos, A. Kotbra, G. Anderson, SAE Int. J. Engines 10 (4) (2017) 1653–1666.
[2] C.P. Cho, Y.D. Pyo, J.Y. Jang, G.C. Kim, Y.J. Shin, Appl. Therm. Eng. 110 (2017) 18–24.
[3] K. Price, J. Jaques, P. Tilly, L. Wang, SAE Int. J. Passeng. Cars - Mech. Syst. 8 (2) (2015) 526–530.
[4] A.F. Ahlström, C.U.I. Odenbrand, Appl. Catal. 60 (1990) 157–172.
[5] S.L. Andersson, P.L.T. Gabrielsson, C.U.I. Odenbrand, AlChE J. 40 (1994) 1911–1919.
[6] R. Khodayari, C.U.I. Odenbrand, Ind. Eng. Chem. Res. 37 (4) (1998) 1196–1202.
[7] B. Hanell, et al., Stiftelsen för Värmeteknisk Forskning, Stockholm, Nr. (1996), p. 558.
[8] H. Kamata, K. Takahashi, C.U.I. Odenbrand, Catal. Lett. 53 (1998) 65–71.
[9] H. Kamata, K. Takahashi, C.U.I. Odenbrand, J. Mol. Catal. A: Chem. 139 (2–3) (1999) 189–198.
[10] C.U.I. Odenbrand, Chem. Eng. Res. Des. 86 (7) (2008) 663–672.
[11] C.U.I. Odenbrand, J.G.M. Brandin, Top. Catal. 60 (2017) 1306–1316.
[12] H. Jung, D.B. Kittelson, M.R. Zachariah, SAE Tech. Pap. (2003) 2003-01-3179.
[13] D. Nicosia, M. Elsener, O. Kröcher, P. Jansohn, Top. Catal. 42–43 (2007) 333–336.
[14] O. Kröcher, M. Elsener, Appl. Catal. B: Environ. 75 (2008) 215–227.
[15] D. Nicosia, I. Czekaj, O. Kröcher, Appl. Catal. B: Environ. 95 (2008) 39–47.
[16] M. Klimczak, P. Kern, T. Heinzelmann, M. Lucas, P. Claus, Appl. Catal. B: Environ. 95 (2010) 39–47.
[17] T. Maunula, T. Kinnunen, M. Iivonen, SAE Tech. Pap. (2011) 2011-01-1316.
[18] International critical tables of numerical data, Physics, Chemistry and Technology 5 Mc Graw-Hill Book Company. Inc., New York, 1928 p. 229.
[19] X. Tang, J. Li, L. Sun, J. Hao, Appl. Catal. B: Environ. 99 (2010) 156–162.
[20] B. Roduit, A. Wokaun, A. Baiker, Ind. Eng. Chem. Res. 37 (1998) 4577–4590.
[21] C.U.I. Odenbrand, Top. Catal. 60 (2017) 1317–1332.
[22] http://www.engineersedge.com/heat_transfer/convective_heat_transfer_coefficients_13378.
[23] Y. Gao, T. Luan, T. Lu, K. Cheng, H. Xu, Chin. J. Chem. Eng. 21 (1) (2013) 1–7.
[24] L.J. Alemany, L. Lietti, N. Ferlazzo, P. Fortzatti, G. Busca, E. Giamello, F. Bregani, J. Catal. 155 (1995) 117–130.
[25] J. Schobing, V. Tschamber, J.F. Brilhac, A. Auclaire, R. Vonarb, Top. Catal. 59 (2016) 1013–1019.
[26] B. Shen, F. Wang, B. Zhao, Y. Li, Y. Wang, J. Ind. Eng. Chem. 33 (2016) 262–269.
[27] S.L. Andersson, P.L.T. Gabrielsson, C.U.I. Odenbrand, AlChE J. 40 (11) (1994) 1911–1919.
[28] M. Koebel, M. Elsener, Chem. Eng. Sci. 53 (4) (1998) 657–669.
[29] F. Tang, B. Xu, H. Shi, J. Qiu, Y. Fan, Appl. Catal. B: Environ. 94 (2010) 71–76.
[30] J.G.M. Brandin, C.U.I. Odenbrand, Catal. Lett. 148 (2018) 312–327.
[31] J.P. Chen, M.A. Buzanowski, R.T. Yang, J.E. Cichanowicz, J. Air Waste Manage. Assoc. 40 (1990) 1403–1409.
[32] D.E. Mears, Ind. Eng. Chem. Process Des. Dev. 10 (4) (1971) 541–547.
[33] D.E. Mears, J. Catal. 20 (1971) 127–131.
[34] D.E. Mears, Ind. Eng. Chem. Fundam. 15 (1) (1976) 20–23.
[35] S. Djerad, M. Crocoll, S. Kureti, L. Tifouti, W. Weisweler, Catal. Today 113 (2006) 208–214.
[36] L. Lietti, I. Nova, P. Forzatti, Top. Catal. 11 (12) (2000) 111–122.
[37] M. Yates, J.A. Martín, M.A. Martín-Luengo, S. Suárez, J. Blanco, Catal. Today 107-108 (2005) 120–125.
[38] B.L. Duffy, H.E. Curry-Hyde, N.W. Cant, P.F. Nelson, J. Phys. Chem. 98 (1994) 7153–7161.
[39] C.U.I. Odenbrand, P.L.T. Gabrielsson, J.G.M. Brandin, L.A.H. Andersson, Appl. Catal. 78 (1991) 109–122.
[40] S. Xiong, X. Xiao, M.A. Martín-Luengo, S. Suárez, J. Blanco, Catal. Today 107–108 (2005) 120–125.